Vol. 128: 203–213, 2018
https://doi.org/10.3354/dao03222

DISEASES OF AQUATIC ORGANISMS
Dis Aquat Org

Published June 4

Generation, characterization and application of monoclonal antibodies against matrix protein of hirame novirhabdovirus (HIRRV) in flounder

Xiaoqian Tang[1,2], Yinghui Qin[1], Xiuzhen Sheng[1], Jing Xing[1,2], Wenbin Zhan[1,2,*]

[1]Laboratory of Pathology and Immunology of Aquatic Animals, KLMME, Ocean University of China, 5 Yushan Road, Qingdao 266003, PR China

[2]Laboratory for Marine Fisheries Science and Food Production Processes, Qingdao National Laboratory for Marine Science and Technology, Qingdao 266235, PR China

ABSTRACT: Hirame novirhabdovirus (HIRRV) causes severe disease in fish cultures, resulting in great economic loss in Asia and Europe. In this study, the matrix protein (M) of HIRRV was recombinantly expressed as the immunogen to produce monoclonal antibodies (MAbs) using hybridoma cell fusion technology, and 3 MAbs were produced and characterized by indirect ELISA, Western blotting and immunofluorescence assay (IFA). Western blotting and mass spectrometric analysis showed that the MAbs could specifically react with the nature M protein of HIRRV. The MAbs were employed to detect virions in HIRRV-infected epithelioma papulosum cyprini (EPC) cells and flounder *Paralichthys olivaceus* by IFA and immunohistochemistry (IHC). In the virus-infected EPC cells, the virions were mainly located in the cytoplasm, whereas in flounder, HIRRV was present in all 10 tested tissues, and the positive signals in spleen, head-kidney and heart were higher than in other tissues, consistent with the results obtained by RT-PCR. Moreover, strong positive signals were observed in the endothelial cells of blood vessels, but only the leukocytes were infected by HIRRV in the whole blood cells. These results indicate that the high susceptibility to HIRRV of leukocytes and endothelial cells may facilitate the spread of HIRRV and finally cause systemic infection in flounder. This study provides a foundation for further studies on rapid diagnosis of HIRRV and its infection mechanisms.

KEY WORDS: Hirame novirhabdovirus · HIRRV · Monoclonal antibody · Matrix protein · Tissue distribution · *Paralichthys olivaceus*

INTRODUCTION

Hirame novirhabdovirus (HIRRV), formerly named Hirame rhabdovirus, is an enveloped negative-strand RNA virus belonging to the genus *Novirhabdovirus* of the family *Rhabdoviridae*. HIRRV was first isolated from moribund Japanese flounder *Paralichthys olivaceus* and ayu *Plecoglossus altivelis* in Japan in 1984 (Kimura et al. 1986). To date, the virus has been found not only in marine fishes, including Japanese flounder (Oh & Choi 1998), stone flounder *Kareius bicoloratus* (Sun et al. 2009), black seabream *Acanthopagrus schlegeli* (Kim & Oh 2015) and sea bass *Lateolabrax maculatus* (Seo et al. 2016), but also in freshwater fishes, such as grayling *Thymallus thymallus* and brown trout *Salmo trutta* (Borzym et al. 2014). Reports on natural and experimental infections showed that HIRRV could cause severe disease symptoms and high mortality in susceptible fishes, posing a great threat to the aquaculture industry (Oseko et al. 1988, Zhang et al. 2017).

Although the glycoprotein subunit vaccine and DNA vaccine are effective in protecting flounder from HIRRV infection experimentally (Eou et al. 2001, Seo et al. 2006), the lack of commercial vaccines or efficient antiviral drugs against HIRRV is still the major difficulty in the control of this viral disease. At present, early diagnosis of viral infection and

*Corresponding author: wbzhan@ouc.edu.cn

timely implementation of measures are still the ideal methods for controlling HIRRV. Therefore, it is necessary to develop rapid and convenient detection methods and to elucidate the infection mechanism of HIRRV. Immunoassays based on specific monoclonal antibodies (MAbs) are more suited to the field detection of viral infections due to their sensitivity, specificity, low cost, speediness and ease of procedures (Wang & Zhan 2006, Wang et al. 2006, Sheng et al. 2012, 2013). MAbs can also be employed as a tool for identifying virus target organs and investigating host–virus interactions and infection mechanisms (Veselý et al. 2004, Ito et al. 2010, Wang et al. 2011). Therefore, specific MAbs against HIRRV are urgently needed. However, no specific anti-HIRRV MAb is currently available.

The HIRRV genome encodes 6 viral proteins in the order of the 3′-leader, i.e. nucleo- (N), phospho- (P), matrix (M), glyco- (G), non-structural (NV), and RNA polymerase (L) protein and the 5′-trailer (Kim et al. 2005, Sun et al. 2011), and their abundances decrease in the above order at both mRNA and protein levels (Banerjee 1987). The M protein of HIRRV is a multifunctional protein essential for virus maturation and budding that also regulates the expression of viral and host proteins, and its content is also higher in virus particles (Lenard & Vanderoef 1990, Graham et al. 2008). In addition, the N and M genes are conserved and are usually employed for phylogenetic and epidemiological studies (Nishizawa et al. 1995). Thus, the M protein is an ideal target for HIRRV detection and an ideal alternative for the generation of MAbs against HIRRV.

In the present study, the M protein of HIRRV was recombinantly expressed and used as the immunogen for MAb production. The produced MAbs were characterized by indirect enzyme-linked immunosorbent assay (ELISA), immunofluorescence assay (IFA) and Western blotting, which were then employed to investigate the distribution of HIRRV in the tissues of infected flounder by IFA and immunohistochemistry (IHC). RT-PCR based on the N gene of HIRRV was also performed to examine the levels of viral loads in different tissues of HIRRV-infected flounder.

MATERIALS AND METHODS

Experimental fish

Apparently healthy flounder, 16–18 cm in body length, were obtained from a fish farm in Qingdao city, Shandong province, China. Prior to the experiment, an RT-PCR assay was performed to confirm that the fish were free of HIRRV. The fish were maintained in aerated running seawater at 10°C and fed commercial pellet food. After acclimating for 2 wk, the fish were used for experiments.

Cell culture and virus purification

Epithelioma papulosum cyprini (EPC) cells were grown at 20°C in medium 199 (M199, Gibco) supplemented with 10% fetal bovine serum (FBS, Gibco), 100 IU ml^{-1} penicillin and 100 µg ml^{-1} streptomycin (Gibco).

HIRRV strain CNPo2015 previously isolated from Japanese flounder was used for the experiment (Zhang et al. 2017). The virus was replicated in EPCs grown in M199 with antibiotics and 2% FBS at 20°C. When the cytopathic effect became extensive, the supernatant was harvested and centrifuged to eliminate cell debris. HIRRV was purified according to the procedure described by Kimura et al. (1986), and purity was checked by sodium dodecyl sulfate polyacrylamide gel electrophoresis (SDS-PAGE).

Expression and purification of recombinant M protein (rM)

Based on the genome sequence of M protein of HIRRV (GenBank No. FJ376982.1), the specific primers (Table 1) were designed to amplify the target gene encoding the M protein. The PCR product of the M gene was purified and digested with the restriction enzymes *Bam*HI and *Sal*I, and then ligased into pET-32a plasmid to construct pET-32a-M recombinant plasmid, which then was transformed into *E. coli* BL21 (DE3). The positive clone was confirmed by sequencing, then incubated in LB medium to a mid-logarithmic phase and induced by adding 0.5 mM isopropyl β-D-1-thiogalactosidase (IPTG). The rM was purified by His Trap™ HP Ni-Agarose (GE Healthcare) following the manufacturer's instructions. The induced bacteria lysate and purified rM were analyzed by SDS-PAGE and visualized after staining with Coomassie brilliant blue R-250. The concentration of rM was determined using the Bradford method.

Production of monoclonal antibodies

Four balb/c mice were immunized intraperitoneally (i.p.) with 100 µl of 1 mg ml^{-1} purified rM protein

Table 1. Primers used in this study. The underlined letters represent the restriction enzyme sites

Primer name	Primer sequence (5′-3′)	Size (bp)
HIRRV-M-F	CGGGATCCATGTCTCTCTTCAAGCGAAC	579
HIRRV-M-R	GCGTCGACTTTCCCCTTTTTGGTTG	579
HIRRV-N-64-F	ATGAGGCTGAGCGGAACC	381
HIRRV-N-444-R	CTTTTTGACCAGAAGGCGAG	381
β-actin-F	AGAGCAAAAGAGGCATCCTGAC	577
β-actin-R	CCGATGGTGATGACCTGGCC	577

emulsified with an equivalent volume of Freund's complete adjuvant (FCA, Sigma). After 2 wk, a similar injection was administrated using Freund's incomplete adjuvant (Sigma) instead of FCA. Booster injections were then given twice via the tail vein at 1 wk intervals. Three days after the last injection, the mice were sacrificed. Spleen cells were collected from the immunized mice and fused with myeloma cells (P3-X63-Ag8U1, P3U1) using 50% polyethylene glycol 4000 (Sigma). The cells were distributed into 96-well culture plates (Costar) in GIT medium (Nihon Seiyaku) supplemented with 1% HAT (Gibco), and the culture medium was changed every 3–5 d. After 12–14 d, the supernatant fluids from those wells growing hybridomas were screened by indirect ELISA. Hybridomas giving positive results were cloned by limiting dilution 3 times, and the MAbs were characterized by indirect ELISA, Western blotting and IFA. Antibodies were produced by injecting hybridomas into the peritoneal cavity of 8 wk old Balb/c mice, and ascetic fluids were obtained within 2 wk.

Specifying MAbs

The specificity of MAbs was detected by indirect ELISA as described by Cheng et al. (2006). Briefly, 100 µl purified rM (20 µg ml^{-1}) was coated into each well of 96-well microplates (Costar) at 4°C overnight, and incubated with hybridoma culture supernatant as primary antibodies, and goat-anti-mouse Ig-alkaline phosphatase conjugate (Sigma) as secondary antibodies for 1 h at 37°C. The myeloma culture supernatant instead of the MAb culture supernatant was added as the negative control. Each experiment was repeated in triplicate.

Western blotting and mass spectrometric analysis

After SDS-PAGE, rM and purified HIRRV were electrophoretically transferred onto a PVDF membrane (Merck Millipore). The MAb or the myeloma culture supernatant and goat anti-mouse Ig-alkaline phosphatase conjugate were then used as primary and secondary antibodies, respectively. Visualization of the antibody-bound proteins was performed according to the method described by Wu et al. (2015). The immune-reactive proteins in HIRRV were excised from polyacrylamide gels and analyzed by an ABI5800 matrix-assisted laser desorption ionization time-of-flight (MALDI-TOF) assay system (Applied Biosystems).

IFA of HIRRV-infected cells

EPC cells were seeded onto cover slips according to the method described by Wu et al. (2015). Briefly, acid-etched circular cover slips were kept in 24-well plates, and 10^5 cells well^{-1} were seeded and incubated to allow cells to attach to the cover slips. After 24 h incubation, the medium was removed and the wells were carefully washed with PBS. Cells were then infected with HIRRV at a multiplicity of infection of 0.1 and incubated at 15°C for 24 h post infection. Monolayers were then rinsed with PBS and fixed with cold acetone for 10 min. After washing with PBS, MAbs were added to glass slides and incubated for 1 h at 37°C in a moisture chamber, and the myeloma culture supernatant instead of the MAbs was added as the negative control. After washing 3 times with PBST, the slides were incubated for 45 min at 37°C in the dark with goat anti-mouse Ig-FITC (1:256, Sigma), and 4,6-diamidino-2-phenylindole (DAPI, Roche) staining (blue) was used to visualize cell nuclei. Slides were rinsed again and then mounted with 50% glycerin and observed under a fluorescence microscope (Olympus DP70).

Virus infection and sampling

For experimental infection, 60 flounder were randomly and equally divided into 2 groups. Each fish in the infection group was intraperitoneally injected with 100 µl culture medium containing $10^{5.5}$ $TCID_{50}$ HIRRV, whereas fish in the control group were injected with the same volume of culture medium without HIRRV. On Day 5 post infection, peripheral blood, liver, spleen, head-kidney, intestine, gill, muscle, brain, heart and stomach were randomly

sampled from 3 fish in the infection and control groups for IFA, IHC and RT-PCR assays. Before handling, the fish were temporarily kept in a water tank containing 100 ng ml^{-1} MS-222 for about 10 min until the respiratory rate of fish was significantly decreased. For euthanasia, the fish were over-anesthetized with 300 ng ml^{-1} of MS-222.

Tissue cryosections and IFA

Tissue cryosections were prepared according to Lin et al. (2007). For IFA, sections were incubated with MAbs against rM (1:1000) and FITC-conjugated goat anti-mouse IgG (1:256, Sigma) containing 1 µg ml^{-1} Evan's blue dye (Fluka) as the counterstain. Incubation with myeloma culture supernatant instead of MAbs against rM was carried out as a negative control. All incubations were conducted at 37°C for 1 h in a moisture chamber in the dark, and slides were washed 3 times with PBST after incubation. The slides were rinsed again and then mounted with 50% glycerin and observed under a fluorescence microscope (Olympus DP70).

Tissue paraffin sections and IHC

IHC was also carried out to investigate the tissue distribution of HIRRV in the HIRRV-infected flounder. Tissue samples were fixed in Bouin's fixative and rinsed with 70% alcohol. Subsequently, the tissues were dehydrated and embedded in paraffin wax, and 6 µm sections were cut using a rotary microtome (Leica) and mounted on poly-L-lysine-coated slides. After dewaxing in xylene and rehydration in graded ethanol, antigen retrieval was carried out as described by Faulk et al. (2014). Sections were pretreated with 0.5 M EDTA for 1 h at room temperature to inhibit endogenous alkaline phosphatase (AP) activity, and blocked with 4% BSA in PBS for 1 h at 37°C. Incubation with mouse anti-rM MAbs diluted 1:1000 in PBS was achieved in a humid chamber for 1 h at 37°C. As controls, the MAbs were replaced by myeloma culture supernatant. After washing 3 times with PBST, the sections were incubated with biotinylated horse anti-mouse IgG (Vector Laboratories) and streptavidinealkaline phosphatase (SA-AP; Boehringer-Mannheim Biochemicals) for 45 min at 37°C, respectively. After washing 3 times with PBST, the slides were incubated with an AP-Red™ substrate kit (Zymed), counterstained with Mayer's hematoxylin for 10 min, mounted with glycerol-PBS (1:1) on glass slides, and examined under a light microscope (Olympus DP70).

Blood cell smear preparation and IFA and IHC

Leukocytes and erythrocytes were isolated from the peripheral blood using a Percoll centrifugation method as a previously reported (Sheng et al. 2015, Xing et al. 2017), and the cells were diluted in PBS to 10^6 cells ml^{-1}. Cells were then settled on glass slides for 2 h, fixed for 10 min with ice-cold acetone and stored at −20°C. The processes of IFA and IHC were the same as described above.

RNA extraction and RT-PCR

In order to further quantify the virus load in different tissues of infected flounder, a semi-quantitative RT-PCR, a more sensitive technique for the detection of HIRRV replication, was carried out. Samples were collected in TRIzol reagent (TaKaRa) and stored at −80°C until use. Total RNA was extracted following the manufacturer's instructions, and RNA was purified using the RNeasy mini kit (TaKaRa) after DNA eraser treatment to remove genomic DNA. The purified RNAs were quantified using a Nanodrop 8000 Spectrophotometer (Thermo Scientific). Total RNA (1 µg) from 3 fish was reverse-transcribed into cDNA using a PrimeScript™ RT reagent Kit (TaKaRa). The cDNA was used as the PCR amplification template with the primers HIRRV-N-64-F and HIRRV-N-444-F (Table 1), which could specifically amplify a part of the N gene of HIRRV. The expected size of the amplified fragment of the N gene was 381 bp. β-actin primers were used as a positive control for PCR to verify the cDNA templates. The primers for β-actin amplification were β-actin-F and β-actin-R (Table 1), and the expected amplified fragment of cDNA was 577 bp long. The reaction was run as follows: denaturing for 5 min at 95°C; 35 cycles of 95°C for 30 s, 57°C for 30 s and 72°C for 45 s; and elongation for 10 min at 72°C. The products were visualized by separation on a 2% agarose gel.

RESULTS

Expression and purification of the M protein

SDS-PAGE revealed that the M protein of HIRRV was successfully expressed in *E. coli* BL21 (DE3) with

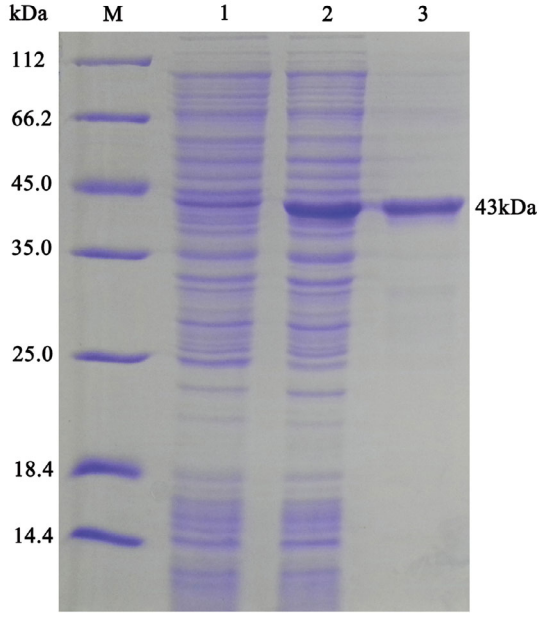

Fig. 1. SDS-PAGE analysis of recombinant matrix protein (rM). Lanes M: molecular mass marker; 1: transformed *E. coli* without IPTG induction; 2: transformed *E. coli* induced with IPTG; 3: purified rM

the pET-32a system after IPTG induction, with a distinct band about 43 kDa (Fig. 1, lane 2), which was in accordance with the predicted molecular mass of fusion recombinant M protein containing approximately 21 kDa His/Trx/S-tag (Tang et al. 2017). After purification with the Ni^{2+} affinity chromatography, rM protein with high purity was obtained (Fig. 1, lane 3).

Production and characteristics of MAbs

A total of 127 hybridomas were observed under an inverted microscope, and 25 of these hybridomas gave positive results compared with myeloma culture supernatant by indirect ELISA. Among the positive cells, the hybridomas with higher absorbance were selected for screening, and 3 MAbs (1F9, 3A6 and 4D10) were finally isolated and cloned by limiting dilution. Isotype determination showed that all 3 MAbs were IgG type. As illustrated in Fig. 2, the results of Western blotting analysis showed that the 3 MAbs could not only react with the recombinant M protein (Fig. 2A), but could also recognize a ~22 kDa protein in HIRRV (Fig. 2B). In contrast, no band was found when MAbs were replaced by myeloma culture supernatant. Mass spectrometry (MS) results showed that 8 mass spectrum peaks (marked with stars) were matched with the M protein of HIRRV. The matched amino acid sequences are underlined in Fig. 3, and the 22 kDa protein matches the M protein of HIRRV with 39% amino acid sequence coverage.

IFA of HIRRV-infected EPC cells

In order to identify whether the MAbs could specifically recognize HIRRV, the IFA of HIRRV-infected cells using produced MAbs was carried out. All 3 antibodies showed strong green fluorescence signals in the HIRRV-infected EPC cells, and specific fluores-

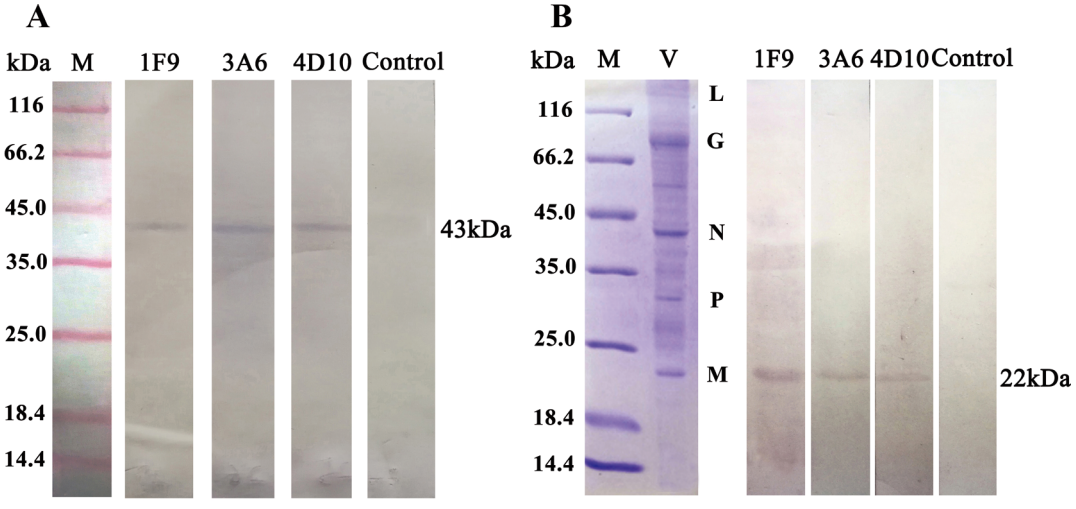

Fig. 2. Western blotting analysis of monoclonal antibodies (MAbs). Lanes M: molecular mass marker; V: purified HIRRV) 1F9: MAb 1F9; 3A6: MAb 3A6; 4D10: MAb 4D10; Control: negative control using myeloma culture supernatant. (A) Western blotting analysis of MAbs with purified recombinant matrix protein. (B) SDS-PAGE and Western blotting analysis of MAbs with purified HIRRV. Also shown are bands for L: RNA polymerase protein; G: glycoprotein; N: nucleoprotein; P: phosphoprotein; M: matrix protein

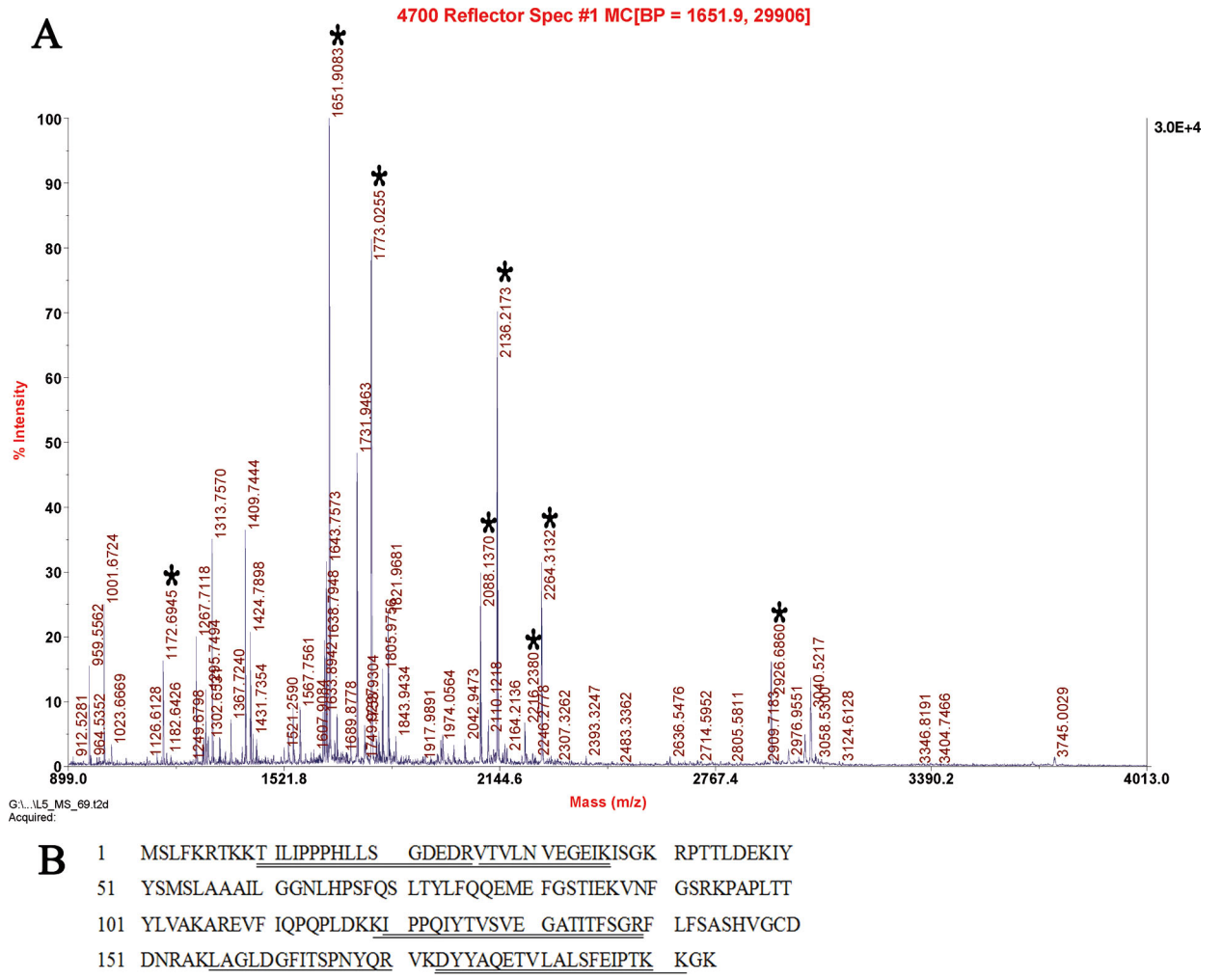

Fig. 3. Mass spectrographic analysis of the 22 kDa protein recognized by 3 MAbs in HIRRV. (A) Fingerprint of the 22 kDa protein; matched peaks are marked with stars. (B) Amino acid sequence of M protein of HIRRV; matched peptides are underlined

cence signals were observed on the cytomembrane and in the cytoplasm. In contrast, no positive signals were observed in the uninfected cells. In addition, DAPI staining showed that the nuclei of HIRRV-infected EPC cells became condensed and small in comparison with the uninfected EPC cells (Fig. 4). These results demonstrate that the MAbs produced could specifically recognize the native form of the M protein in HIRRV-infected cells, which could be further used to identify the target organs and tissues of HIRRV in flounder.

Tissue distribution of HIRRV in infected flounder (IFA)

IFA using MAbs against the M protein of HIRRV was carried out to examine the tissue distribution of HIRRV in infected flounder. Evident green fluorescence signals, indicating the existence of HIRRV, were observed in all 10 investigated tissues. According to the positive signals observed, HIRRV was mainly located in liver hepatocytes, serosa and white pulp surrounding ellipsoids of the spleen, epithelial cells of the anterior renal tubules, mucosal epithelium and muscle layer and endothelial cells of blood vessels of intestine, gill epidermis, muscle fibers, glial cells in the granular layer and endothelial cells of blood vessels of brain, cardiac cells, lamina propria of stomach mucosa and gastric gland epithelium. No positive signal was observed in negative controls (Fig. 5). Interestingly, strong green fluorescence signals were present in leukocytes (Fig. 5J) and the endothelial cells of blood vessels (Fig. 6), but not in the erythrocytes (Fig. 5J′). All tested tissues were counterstained by Evans blue dye and appeared bright red.

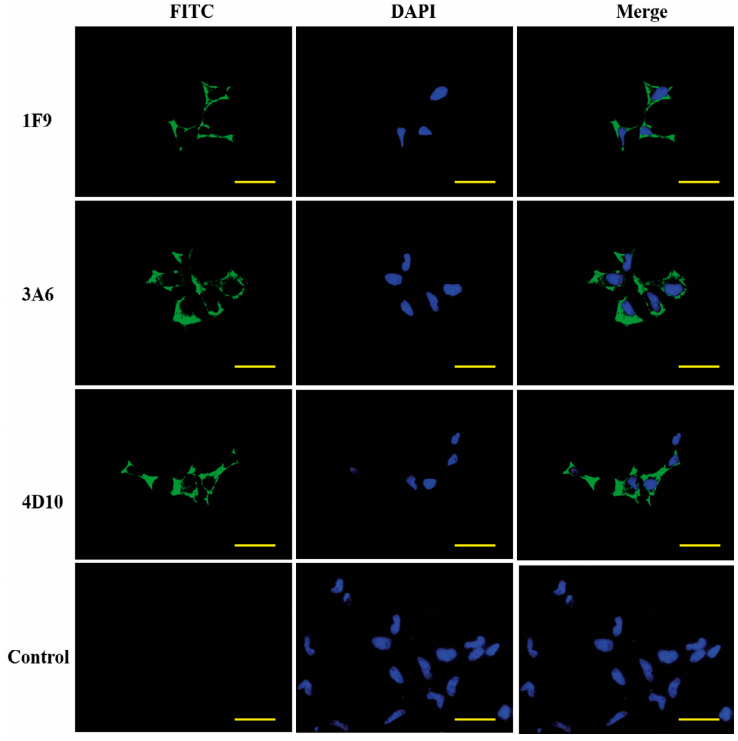

Fig. 4. IFA of HIRRV-infected EPC cells with 3 MAbs (1F9, 3A6 and 4D10). Nuclei were stained with DAPI, showing blue fluorescence. Green fluorescence signals in the cytoplasm of infected cells indicate the existence of HIRRV. Scale bars = 20 µm

Tissue distribution of HIRRV in infected flounder (IHC)

In order to further determine the target organs and tissues for HIRRV, IHC analysis was performed using the anti-rM MAbs. Findings were consistent with the results obtained by IFA, in that positive red signals were also observed in all 10 tested tissues, showing the existence of HIRRV. No red positive signal was observed in the negative controls. Strong positive signals were present in leukocytes, but no positive signals were observed in erythrocytes. All tested tissues were counterstained with Mayer's hematoxylin (Fig. 6).

Tissue distribution of HIRRV in infected flounder (RT-PCR assay)

The results of the semi-quantitative RT-PCR assay revealed HIRRV in all examined tissues. The highest level of HIRRV was present in the spleen, head-kidney, heart and blood, followed by

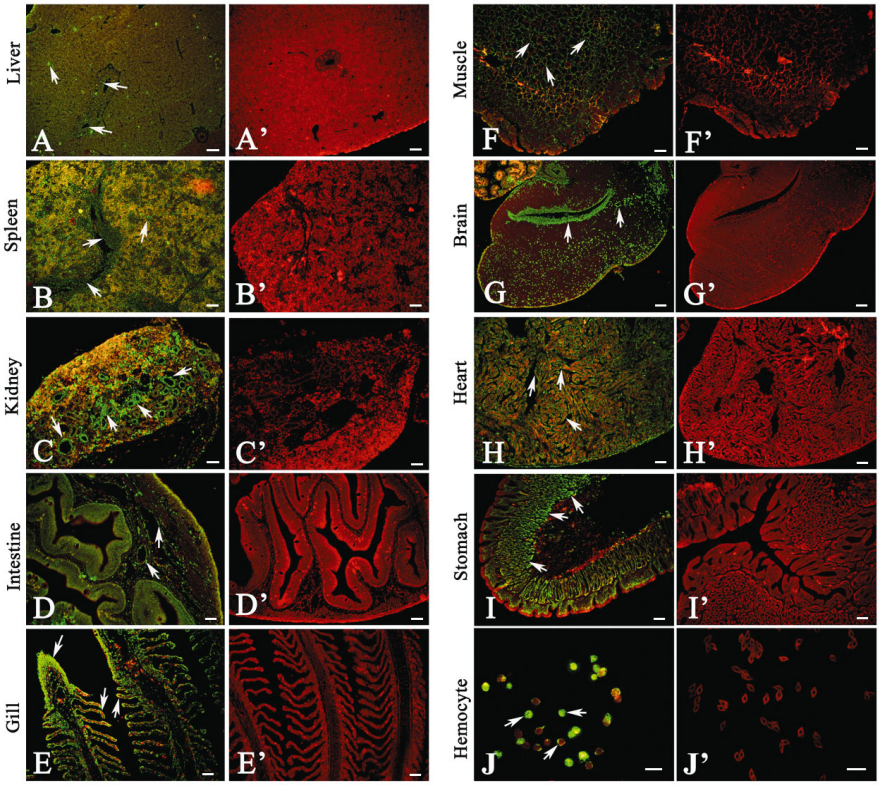

Fig. 5. Tissue distribution of HIRRV in infected flounder, detected by IFA. Green fluorescence (arrows) indicates positive signals of HIRRV. (A–I) Experimental groups: liver (A), spleen (B), head-kidney (C), intestine (D), gill (E), muscle (F), brain (G), heart (H), stomach (I), leukocytes (J), erythrocytes (J') were incubated with anti-rM MAbs. (A'–I') Negative control groups were incubated with myeloma culture supernatant. All tissues were counterstained in red with Evan's blue dye. Scale bars = 50 µm

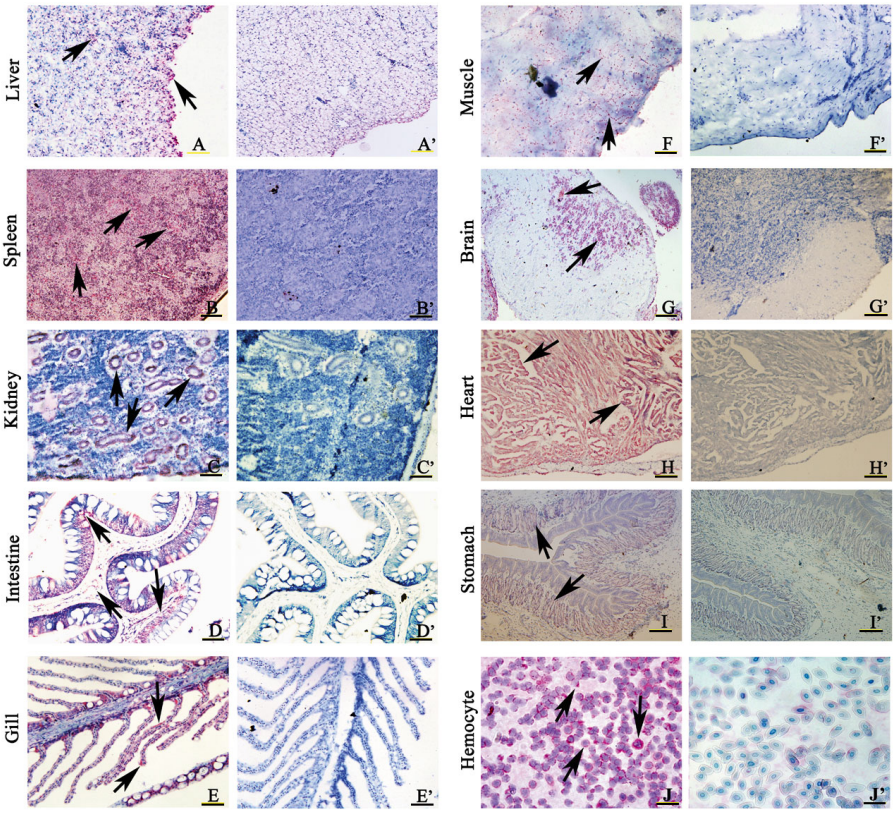

Fig. 6. Immunohistochemical detection of HIRRV in the tissues of infected flounder. (A–I) Red positive signals (arrows) were observed in experimental groups: liver (A), spleen (B), head-kidney (C), intestine (D), gill (E), muscle (F), brain (G), heart (H), stomach (I), leukocytes (J) and erythrocytes (J′). (A′–I′) No red positive signal is visible in negative control groups, which were incubated with myeloma culture supernatant as the primary antibody. All tissues were counterstained with Mayer's hematoxylin. Scale bars = 20 µm

brain, liver and muscle, and then the intestine, gill and stomach (Fig. 7).

DISCUSSION

HIRRV is an important pathogen of both marine and freshwater fish and has resulted in enormous economic losses in Asia and Europe (Borzym et al. 2014, Zhang et al. 2017). The high pathogenicity, together with nonavailability of commercial vaccines or drugs against HIRRV, highlights the urgent need to develop simple and rapid diagnostic methods. Unfortunately, research on HIRRV is far from sufficient, and no available antibodies have been reported up to now. Therefore, it is significant to produce specific MAbs against HIRRV for the development of rapid diagnosis methods and investigation of infection mechanisms of HIRRV. However, traditional MAb production methods require abundant high-purity virus particles, which are extremely difficult to obtain (Cheng et al. 2006, Zhou et al. 2008). Moreover, the produced MAbs using purified virus particles as immunogens are liable to react with the abundant proteins in the virus. Therefore, in the present study, the high-purity rM of HIRRV was used as the immunogen for MAb production, and 3 MAbs specific to HIRRV were obtained. ELISA and Western blotting both showed that the 3 MAbs could react with rM. Moreover, a 22 kDa protein in HIRRV was recognized by the 3 MAbs in a Western blotting assay, which was identified to be the M protein of HIRRV by MS analysis. Furthermore, IFA showed that HIRRV-positive signals were only detected in the membrane and cytoplasm of HIRRV-infected EPCs. This result was well supported by previous studies, which showed that novirhabdovirus replication sites occur in the cytoplasm that acts as a virus 'factory,' and the viruses undergo morphogenesis from cytoplasmic membranes (Kristensson et al. 1996, Zhou et al. 2008). In addition, Zhang et al.

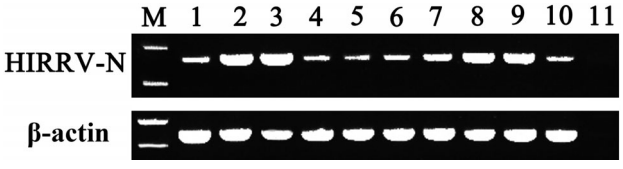

Fig. 7. Distribution of HIRRV in various tissues of infected flounder as determined by RT-PCR of the N gene of HIRRV. Lanes M: marker; 1: liver; 2: spleen; 3: head-kidney; 4: intestine; 5: gill; 6: muscle; 7: brain; 8: heart; 9: blood; 10: stomach; 11: blank control without cDNA

(2017) observed that abundant HIRRV particles were aggregated on the surface of EPCs, and some HIRRV bodies presented in the cytoplasm of EPCs by transmission electron microscopy. Therefore, our results demonstrated that the developed MAbs could react with recombinant and native M protein of HIRRV, suggesting that the recognized epitopes were linear and conformation-independent. In addition, we also found that the nuclei of virus-infected cells became condensed and small, which is in accordance with previous research (Zhou et al. 2006, Chen et al. 2008, Zhang et al. 2017).

Tissue distribution and the sites of replication are fundamental in understanding pathogenesis of a virus. For most viruses, the viral amounts often vary in different tissues and appear higher in susceptible tissues, which are considered potential targets for virus detection (Jiravanichpaisal et al. 2004, Wang & Zhan 2006). In our preliminary experiment, obvious symptoms (reddened fins and expanded abdomen) were developed at 5 d post infection, when mortality of HIRRV-infected flounder began to occur (Zhang et al. 2017). This was the reason why we chose the time point to study the tissue distribution of HIRRV. In this study, HIRRV particles could be detected in all 10 tested tissues of HIRRV-infected flounder, suggesting that HIRRV causes a systemic infection in flounder. RT-PCR indicated that the virus load was relatively higher in spleen, head-kidney, heart and peripheral blood, followed by brain, liver and muscle, and lower in intestine, gill and stomach. Previous research found that the spleen and kidney pools of HIRRV-infected flounder had the highest virus titer (Kimura et al. 1986). In grass carp infected with *Paralichthys olivaceus* rhabdovirus (PORV), the spleen and kidney also showed stronger positive immunostaining in comparison with liver and gill (Zhou et al. 2008). Similar distribution patterns were also observed in diseased fish infected by other novirhabdoviruses (Yamamoto et al. 1990, Romero et al. 2005). These results suggested that the infection of HIRRV in flounder eventually resulted in a systemic disease, and the hematopoietic organs (spleen and head-kidney) and heart might be the major infection targets of HIRRV.

Endothelial cells contain a number of surface receptors that play critical roles in the regulation of immune cell adherence, capillary permeability, complement activation and immune responses, which could be altered by virus infection and contribute to hemorrhage or edema (Mackow & Gavrilovskaya 2009). In this study, we also found that HIRRV could infect epithelial cells of numerous organs, and strong positive signals of HIRRV were present in the endothelial cells of blood vessels of infected tissues but not in the extravascular and intravascular erythrocytes. Previous studies showed that the major clinical sign of HIRRV-infected fish was septicemia, which is manifested as severe bleeding of the internal organs (Kimura et al. 1986, Zhang et al. 2017). Similar phenomena also are found in diseased fish infected by other novirhabdoviruses. Evensen et al. (1994) found that viral hemorrhagic septicemia virus (VHSV) was present primarily in the endothelial cells lining venules and sinusoids of numerous tissues of diseased rainbow trout, and the presence of virus was accompanied by cell degeneration and necrosis in all infected organs. Al-Hussinee et al. (2011) reported that all VHSV-infected fish in their study had dramatic vasculitis, and abundant VHSV was detected within the cytoplasm of endothelial cells of blood vessels in infected tissues. These results suggest that HIRRV has a distinct tropism for endothelial cells of blood vessels, and its degeneration and necrosis is mainly responsible for the septicemia of infected flounder. Interestingly, strong positive signals were also observed in a portion of leukocytes in HIRRV-infected flounder, but not in the erythrocytes. Similarly, strong VHSV-positive signals were present in scattered intact and necrotic leukocytes and intravascular leukocytes within infected tissues (Al-Hussinee et al. 2011). Drolet et al. (1994) reported that infectious hematopoietic necrosis virus-positive cells in hemorrhaged blood pools were primarily macrophages, with no red blood cell involvement. Considering the virus distribution and viral load in different tissues, leukocytes may be the targets and may play important roles in the transmission of HIRRV in flounder. Further studies are needed to determine which subset of the leukocytes could be infected by HIRRV.

In conclusion, this is the first study to produce MAbs against HIRRV and to systematically investigate the tissue distribution of HIRRV in diseased flounder. Our results show that these MAbs specifically recognize the nature M protein in HIRRV. Based on the MAbs, higher quantities of HIRRV were detected in spleen, kidney and heart, and strong HIRRV positive signals were present in the leukocytes and endothelial cells of blood vessels. All resultant data provide a foundation for further studies on the rapid diagnosis and infection mechanisms of HIRRV.

Acknowledgements. This study was supported by the National Natural Science Foundation of China (31730101, 31672685, 31672684, 31472295), Taishan Scholar Program of

Shandong Province, and the Open Foundation of Functional Laboratory for Marine Fisheries Science and Food Production Processes, Qingdao National Laboratory for Marine Science and Technology (2016LMFS-A01).

LITERATURE CITED

Al-Hussinee L, Lord S, Stevenson RMW, Casey RN and others (2011) Immunohistochemistry and pathology of multiple Great Lakes fish from mortality events associated with viral hemorrhagic septicemia virus type IVb. Dis Aquat Org 93:117–127

Banerjee AK (1987) Transcription and replication of rhabdoviruses. Microbiol Rev 51:66–87

Borzym E, Matras M, Maj-Paluch Baud M, Boisséson C, Talbi C, Olesen NJ, Bigarré L (2014) First isolation of hirame rhabdovirus from freshwater fish in Europe. J Fish Dis 37:423–430

Chen ZY, Liu H, Li ZQ, Zhang QY (2008) Development and characterization of monoclonal antibodies to spring viraemia of carp virus. Vet Immunol Immunopathol 123: 266–276

Cheng S, Zhan W, Xing J, Sheng X (2006) Development and characterization of monoclonal antibody to the lymphocystis disease virus of Japanese flounder *Paralichthys olivaceus* isolated from China. J Virol Methods 135: 173–180

Drolet BS, Rohovec JS, Leong JC (1994) The route of entry and progression of infectious haematopoietic necrosis virus in *Oncorhynchus mykiss* (Walbaum): a sequential immunohistochemical study. J Fish Dis 17:337–344

Eou JI, Oh MJ, Jung SJ, Song YH, Choi TJ (2001) The protective effect of recombinant glycoprotein vaccine against HIRRV infection. Fish Pathol 36:67–72

Evensen Ø, Meier W, Wahli T, Olesen NJ, Vestergård Jørgensen PE, Håstein T (1994) Comparison of immunohistochemistry and virus cultivation for detection of viral haemorrhagic septicaemia virus in experimentally infected rainbow trout *Oncorhynchus mykiss*. Dis Aquat Org 20:101–109

Faulk DM, Carruthers CA, Warner HJ, Kramer CR, Reing JE, Amore AD, Badylak SF (2014) The effect of detergents on the basement membrane complex of a biologic scaffold material. Acta Biomater 10:183–193

Graham SC, Assenberg R, Delmas O, Verma A and others (2008) Rhabdovirus matrix protein structures reveal a novel mode of self-association. PLOS Pathog 4:e1000251

Ito T, Olesen NJ, Skall HF, Sano M, Kurita J, Nakajima K, Iida T (2010) Development of a monoclonal antibody against viral haemorrhagic septicaemia virus (VHSV) genotype IVa. Dis Aquat Org 89:17–27

Jiravanichpaisal P, Söderhäll K, Söderhäll I (2004) Effect of water temperature on the immune response and infectivity pattern of white spot syndrome virus (WSSV) in freshwater crayfish J. Fish Shellfish Immunol 17:265–275

Kim DH, Oh HK, Eou JI, Seo HJ and others (2005) Complete nucleotide sequence of the hirame rhabdovirus, a pathogen of marine fish. Virus Res 107:1–9

Kim WS, Oh MJ (2015) Hirame rhabdovirus (HIRRV) as the cause of a natural disease outbreak in cultured black seabream (*Acanthopagrus schlegeli*) in Korea. Arch Virol 160:3063–3066

Kimura T, Yoshimizu M, Gorie S (1986) A new rhabdovirus isolated in Japan from cultured hirame (Japanese flounder) *Paralichthys olivaceus* and ayu *Plecoglossus altivelis*. Dis Aquat Org 1:209–217

Kristensson K, Dasturt DK, Manghanit DK, Tsiangt H, Bentivoglio M (1996) Rabies: interactions between neurons and viruses. A review of the history of Negri inclusion bodies. Neuropathol Appl Neurobiol 22:179–187

Lenard J, Vanderoef R (1990) Localization of the membrane-associated region of vesicular stomatitis virus M protein at the N terminus, using the hydrophobic, photoreactive probe 125I-TID. J Virol 64:3486–3491

Lin Y, Zhan W, Li Q, Zhang Z, Wei X, Sheng X (2007) Ontogenesis of haemocytes in shrimp (*Fenneropenaeus chinensis*) studied with probes of monoclonal antibody. Dev Comp Immunol 31:1073–1081

Mackow ER, Gavrilovskaya IN (2009) Hantavirus regulation of endothelial cell functions. Thromb Haemost 102: 1030–1041

Nishizawa T, Kurath G, Winton JR (1995) Nucleotide sequence of the 2 matrix protein genes (M1 and M2) of hirame rhabdovirus (HRV), a fish rhabdovirus. Vet Res 26:408–412

Oh MJ, Choi TJ (1998) A new rhabdovirus (HRV-like) isolated in Korea from cultured Japanese flounder *Paralichthys olivaceus*. J Fish Pathol 11:129–136

Oseko N, Yoshimizu M, Kimura T (1988) Effect of water temperature on artificial infection of Rhabdovirus olivaceus (hirame rhabdovirus: HRV) to hirame (Japanese flounder, *Paralichthys olivaceus*). Fish Pathol 23:125–132

Romero A, Figueras A, Tafalla C, Thoulouze MI, Bremont M, Novoa B (2005) Histological, serological and virulence studies on rainbow trout experimentally infected with recombinant infectious hematopoietic necrosis viruses. Dis Aquat Org 68:17–28

Seo HG, Do JW, Jung SH, Han HJ (2016) Outbreak of hirame rhabdovirus infection in cultured spotted sea bass *Lateolabrax maculatus* on the western coast of Korea. J Fish Dis 39:1239–1246

Seo JY, Kim KH, Kim SG, Oh MJ, Nam SW, Kim YT, Choi TJ (2006) Protection of flounder against hirame rhabdovirus (HIRRV) with a DNA vaccine containing the glycoprotein gene. Vaccine 24:1009–1015

Sheng XZ, Song JL, Zhan WB (2012) Development of a colloidal gold immunochromatographic test strip for detection of lymphocystis disease virus in fish. J Appl Microbiol 113:737–744

Sheng X, Xu X, Zhan W (2013) Development and application of antibody microarray for lymphocystis disease virus detection in fish. J Virol Methods 189:243–249

Sheng X, Wu R, Tang X, Xing J, Zhan W (2015) Tissue localization of lymphocystis disease virus (LCDV) receptor-27.8 kDa and its expression kinetics induced by the viral infection in turbot (*Scophthalmus maximus*). Int J Mol Sci 16:26506–26519

Sun YJ, Jiang YL, Liu H, Gao LY, Shi XJ, He JQ, Wang Z (2009) The isolation and characterization of a rhabdovirus from stone flounder, *Kareius bicoloratus*. Chin J Vet Sci 29:277–282

Sun Y, Zhang M, Lou H, Wang Z (2011) Analysis and characterization of the complete genomic sequence of the Chinese strain of hirame rhabdovirus. J Fish Dis 34: 167–171

Tang X, Liu F, Sheng X, Xing J, Zhan W (2017) Production, characterization and application of monoclonal antibody against immunoglobulin D heavy chain of flounder (*Paralichthys olivaceus*). Fish Shellfish Immunol 64:401–406

Veselý T, Nevoránková Z, Hulová J, Reschová S, Pokorová D (1993) Monoclonal antibodies to nucleoprotein and glycoprotein of the virus of infectious haematopoietic necrosis of salmonids (IHNV) and their use in immunoperoxidase test. Prog Brain Res 98:309–315

Wang M, Sheng XZ, Xing J, Tang XQ, Zhan WB (2011) Identification of a 27.8 kDa protein from flounder gill cells involved in lymphocystis disease virus binding and infection. Dis Aquat Org 94:9–16

Wang X, Zhan W (2006) Development of an immunochromatographic test to detect white spot syndrome virus of shrimp. Aquaculture 255:196–200

Wang X, Zhan W, Xing J (2006) Development of dot-immunogold filtration assay to detect white spot syndrome virus of shrimp. J Virol Methods 132:212–215

Wu R, Tang X, Sheng X, Zhan W (2015) Relationship between expression of cellular receptor-27.8 kDa and lymphocystis disease virus (LCDV) infection. PLOS ONE 10:e0127940

Xing J, Xiao YE, Tang XQ, Sheng XZ, Zhan WB (2017) Inhibition of cyclosporine A or rapamycin on T lymphocyte counts and the influence on the immune responses of B lymphocytes in flounder (*Paralichthys olivaceus*). Fish Shellfish Immunol 66:78–85

Yamamoto T, Batts WN, Arakawa CK, Winton JR (1990) Multiplication of infectious hematopoietic necrosis virus in rainbow trout following immersion infection: whole-body assay and immunohistochemistry. J Aquat Anim Health 2:271–280

Zhang J, Tang X, Sheng X, Xing J, Zhan W (2017) Isolation and identification of a new strain of hirame rhabdovirus (HIRRV) from Japanese flounder *Paralichthys olivaceus* in China. Virol J 14:73

Zhou GZ, Li ZQ, Zhang QY (2006) Characterization and application of monoclonal antibodies against turbot (*Scophthalmus maximus*) rhabdovirus. Viral Immunol 19:637–645

Zhou GZ, Gui L, Li ZQ, Yuan XP, Zhang QY (2008) Generation and characterization of monoclonal antibodies against the flounder *Paralichthys olivaceus* rhabdovirus. J Virol Methods 148:205–210

Editorial responsibility: James Jancovich, San Marcos, California, USA

Submitted: December 12, 2017; Accepted: March 13, 2018
Proofs received from author(s): May 14, 2018